

Dalton Transactions

Accepted Manuscript



This is an *Accepted Manuscript*, which has been through the Royal Society of Chemistry peer review process and has been accepted for publication.

Accepted Manuscripts are published online shortly after acceptance, before technical editing, formatting and proof reading. Using this free service, authors can make their results available to the community, in citable form, before we publish the edited article. We will replace this *Accepted Manuscript* with the edited and formatted *Advance Article* as soon as it is available.

You can find more information about *Accepted Manuscripts* in the [Information for Authors](#).

Please note that technical editing may introduce minor changes to the text and/or graphics, which may alter content. The journal's standard [Terms & Conditions](#) and the [Ethical guidelines](#) still apply. In no event shall the Royal Society of Chemistry be held responsible for any errors or omissions in this *Accepted Manuscript* or any consequences arising from the use of any information it contains.

ARTICLE

Syntheses and Properties of Phosphine-Substituted Ruthenium(II) Polypyridine Complexes with Nitrogen Oxides

Cite this: DOI: 10.1039/x0xx00000x

Received 00th January 2012,
Accepted 00th January 2012

DOI: 10.1039/x0xx00000x

www.rsc.org/

Go Nakamura,^{ab} Mio Kondo,^{abcd} Meredith Crisalli,^e Sze Koon Lee,^a Akane Shibata,^a Peter C. Ford,^e and Shigeyuki Masaoka^{*abd}

Four novel phosphine-substituted ruthenium(II) polypyridine complexes with nitrogen oxides—*trans*(*P*,*NO*₂)-[Ru(trpy)(Pqn)(NO₂)]PF₆ (*trans*-**NO**₂), *cis*(*P*,*NO*₂)-[Ru(trpy)(Pqn)(NO₂)]PF₆ (*cis*-**NO**₂), [Ru(trpy)(dppbz)(NO₂)]PF₆ (**PP**-**NO**₂), and *cis*(*P*,*NO*)-[Ru(trpy)(Pqn)(NO)](PF₆)₃ (*cis*-**NO**)—were synthesised (trpy = 2,2',6',2''-terpyridine, Pqn = 8-(diphenylphosphanyl)quinoline, and dppbz = 1,2-bis(diphenylphosphanyl)benzene). The influence of the number and position of the phosphine group(s) on the electronic structure of these complexes was investigated using single-crystal X-ray structural analysis, UV-vis absorption spectroscopy, and electrochemical measurements. The substitution lability of the nitrogen oxide ligand of each complex is discussed in comparison with that of the corresponding acetonitrile complexes.

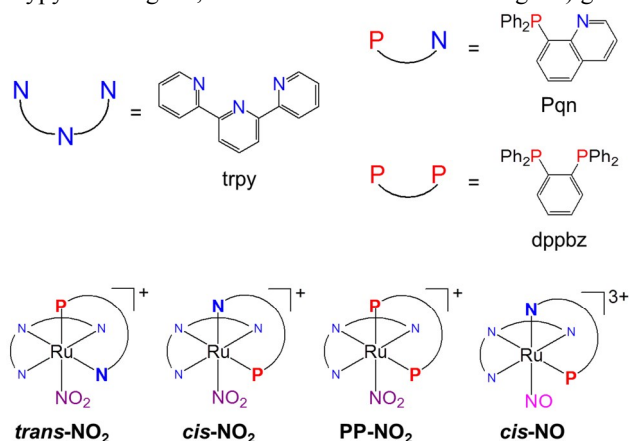
Introduction

Ruthenium(II) polypyridine complexes are widely studied materials because of their contributions to fundamental coordination chemistry, including electrochemistry, photochemistry, and photophysics,¹ and their potential applications in energy conversion,² luminescent sensors,³ electroluminescence displays,⁴ and biotechnology.⁵ Of particular interest are the Ru(II) complexes [Ru(TL)(BL)(L)]ⁿ⁺ (TL = tridentate polypyridine ligand, BL = bidentate polypyridine ligand, and L = monodentate labile ligand) given

their catalytic activity for various reactions, such as oxidation,^{6,7} reduction,⁸⁻¹¹ and photo-induced reactions.¹²

Phosphine-containing ruthenium(II) complexes are also attractive for potential applications in energy conversion systems¹³ and catalysis¹⁴⁻¹⁷ owing to the σ -donating and π -accepting abilities of the phosphine ligands. Thus, it should be possible to develop ruthenium complexes that have novel and tunable properties and reactivity by designing mixed polypyridyl/phosphine complexes. There have been several reports on the syntheses of ruthenium(II) polypyridine complexes containing monodentate phosphine ligands^{18,19} and their catalytic activities^{19d,20}. However, ruthenium(II) polypyridine complexes of the type [Ru(TL)(BL)(L)]ⁿ⁺ bearing bidentate ligands with P and N donors have not been investigated.

In our previous report,²¹ we synthesised and structurally characterised for the first time a series of phosphine-containing ruthenium(II) polypyridine complexes of the type [Ru(TL)(BL)(L)]ⁿ⁺, with L = acetonitrile, TL = 2,2':6',2''-terpyridine (trpy), and BL = 8-(diphenylphosphanyl)quinoline (Pqn) or 1,2-bis(diphenylphosphanyl)benzene (dppbz) (Scheme 1). The influence of the number and position of phosphine donors on the structures and electronic properties was characterised, and unique isomerisation behaviours of these complexes were observed. The coordinating phosphorous ligands played a crucial role in these isomerisation reactions, and the results encouraged us to investigate in more detail the



Scheme 1 Structures of a tridentate ligand (trpy), bidentate ligands (Pqn and dppbz), and metal complexes (*trans*-**NO**₂, *cis*-**NO**₂, **PP**-**NO**₂, and *cis*-**NO**) used in this study.

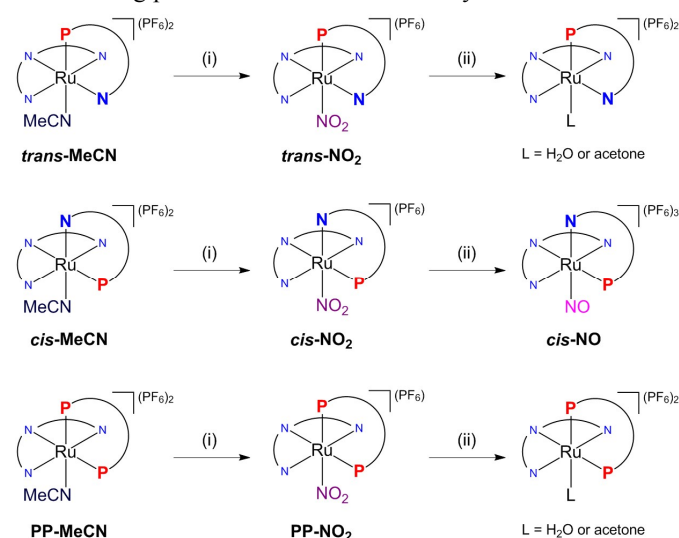
influence of the P atom on the physical properties of Ru-based metal complexes.

In this study, we investigated the reaction of phosphine-containing ruthenium complexes with the nitrogen oxides, NO and NO₂[−], because of their biological roles as signalling molecules²² and reservoirs,²³ in addition to the fundamental interest in their coordination chemistry. Here, we show the syntheses, structural characterisation, and electrochemical and spectroscopic properties of a series of ruthenium(II) polypyridine complexes containing Pqn or dppbz with nitric oxides. Three novel nitrito-κN complexes—*trans*(P,NO₂)- and *cis*(P,NO₂)-[Ru(trpy)(Pqn)(NO₂)]PF₆ (*trans*-NO₂ and *cis*-NO₂), and [Ru(trpy)(dppbz)(NO₂)]PF₆ (**PP**-NO₂)—were successfully synthesised. Described here are the single-crystal X-ray structural determinations, UV-vis absorption spectra, and electrochemical measurements for these complexes, and the preparation of the nitrosyl complex *cis*(P,NO)-[Ru(trpy)(Pqn)(NO)](PF₆)₃ (*cis*-NO) from *cis*-NO₂ and its properties are examined. The present study allows us to probe systematically the chemical and structural properties of phosphine-containing ruthenium complexes with nitrogen oxides by the use of the geometric isomers of the Pqn complex. Additionally, other reactivity properties and comparisons with those of the corresponding acetonitrile complexes are presented.

Results and discussion

Syntheses and Characterisation

The synthetic procedures to obtain *trans*-NO₂, *cis*-NO₂, and **PP**-NO₂ are shown in Scheme 2. The precursors, *trans*-MeCN, *cis*-MeCN, and **PP**-MeCN, were synthesised according to the method that we previously reported.²¹ The reaction of the respective acetonitrile complexes with excess NaNO₂ in a 1:1 mixture of ethanol:water at 100°C gave the corresponding nitrito-κN complexes (*trans*-NO₂, *cis*-NO₂, and **PP**-NO₂).^{24,26b} The resulting products were characterised by ¹H NMR and



Scheme 2 Syntheses of *trans*-NO₂, *cis*-NO₂, **PP**-NO₂, and *cis*-NO. (i) NaNO₂ in 1:1 mixture of ethanol:water at 100°C. (ii) HPF₆ in acetone at 0°C.

³¹P{¹H} NMR spectroscopy and elemental analysis.

The ³¹P{¹H} NMR spectra of *trans*-NO₂ and *cis*-NO₂ in CD₃CN displayed singlets at δ 53.10 and 54.06, respectively, showing upfield shifts (Δδ = 5.70 and 1.90) compared to the spectra of the corresponding acetonitrile complexes, *trans*-MeCN and *cis*-MeCN (δ 58.80 and 55.96). The ³¹P{¹H} NMR spectrum of **PP**-NO₂ in CD₃CN afforded two doublets at δ 62.65 and 68.59 with coupling constants of 14.2 Hz, again showing upfield shifts (Δδ = 5.85 and 1.18, respectively) compared with the spectrum of **PP**-MeCN (68.57 and 69.77, ²J_{P-P} = 20.2 Hz).

Conversions of the nitrito-κN complexes to the corresponding ruthenium nitrosyls were attempted by adding an excess of HPF₆ to acetone solutions of the nitrito-κN species at 0°C. The preparations of *trans*-NO and **PP**-NO from *trans*-NO₂ and **PP**-NO₂, respectively, were not successful because of the instability of the nitrosyl complex or of a reaction intermediate under acidic conditions (for details, see Figures S1-2 in the ESI). However, *cis*-NO was isolated in 85% yield and was characterised by ¹H and ³¹P{¹H} NMR spectroscopy and elemental analysis. The ³¹P{¹H} NMR spectrum of *cis*-NO in acetone-*d*₆ gave a singlet at δ 54.23. *cis*-NO immediately converted to a solvent-coordinated complex in acetonitrile (Figure S3 in the ESI) but was meta-stable in weaker-coordinating solvents, such as acetone, γ-butyrolactone and ethylene glycol (Figure S4 in the ESI). The difference in the stability of these nitrosyl complexes will be discussed in the “Substitution Lability of Nitrogen Oxide” section.

Crystal Structures

Single crystals of *trans*-NO₂ and **PP**-NO₂ suitable for structural

Table 1 Crystallographic data for *trans*-NO₂, *cis*-NO₂, and **PP**-NO₂.

Complex	<i>trans</i> -NO ₂ ·CH ₃ CN	<i>cis</i> -NO ₂ ·0.5CH ₃ CN	PP -NO ₂ ·2CH ₃ OH
Formula	C ₃₈ H ₃₀ F ₆ N ₆ O ₂ P ₂ Ru	C ₆₁ H _{48.5} BN _{5.5} O ₂ PRu	C ₄₇ H ₄₃ F ₆ N ₄ O ₄ P ₃ Ru
Formula weight	879.69	1033.40	1035.83
Crystal colour, habit	red, needle	orange-red, platelet	orange, block
Crystal system	monoclinic	triclinic	monoclinic
Crystal size, mm ³	0.30 × 0.05 × 0.05	0.15 × 0.15 × 0.10	0.15 × 0.10 × 0.05
Space group	P2 ₁ /n	P1̄	P2 ₁ /c
<i>a</i> , Å	12.1909(17)	10.2764(2)	17.1049(6)
<i>b</i> , Å	11.9003(17)	21.2343(4)	13.0763(6)
<i>c</i> , Å	25.260(4)	24.3802(4)	20.1547(8)
α, °	90	77.0060(10)	90
β, °	99.579(3)	78.9530(10)	106.853(3)
γ, °	90	74.9360(10)	90
<i>V</i> , Å ³	3613.5(9)	4955.30(16)	4314.4(3)
<i>Z</i>	4	4	4
<i>D</i> _{calc} , g cm ^{−3}	1.617	1.385	1.595
μ, mm ^{−1}	0.599	0.400	0.552
<i>F</i> (000)	1776	2132	2112
<i>R</i> ₁ ^a	0.0596	0.0337	0.0397
<i>wR</i> ₂ ^b	0.1678	0.1071	0.0941
Goodness-of-fit <i>S</i>	1.032	1.178	1.004

[a] *R*₁ = Σ||*F*_o|| − ||*F*_c|| / Σ||*F*_o||. [b] *wR*₂ = [Σ(*w*(*F*_o² − *F*_c²)²) / Σ*w*(*F*_o²)²]^{1/2}

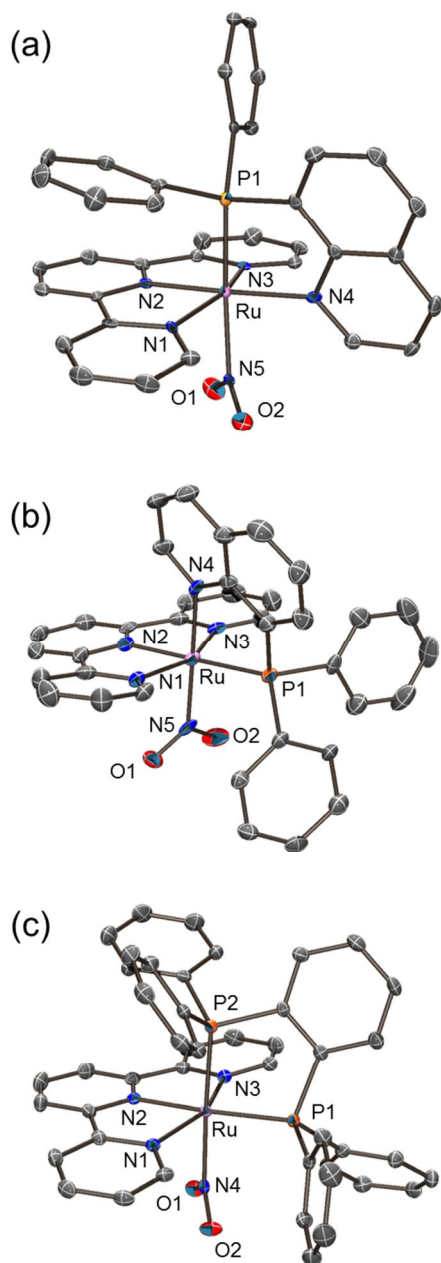


Figure 1 ORTEP drawings (50% probability level) of cationic complexes in (a) *trans*-NO₂, (b) *cis*-NO₂', and (c) PP-NO₂. Hydrogen atoms are omitted for clarity.

determination were obtained by recrystallisation from diethyl ether/methanol/acetonitrile. Single crystals of the *cis*-nitrito-κ*N* complex were obtained as the BPh₄[−] salt, *cis*(*P*,NO₂)-[Ru(trpy)(Pqn)(NO₂)]BPh₄ (*cis*-NO₂'), by adding an excess of NaBPh₄, instead of NH₄PF₆, after the reaction. The molecular structures of *trans*-NO₂, *cis*-NO₂', and PP-NO₂ determined by single-crystal X-ray crystallography and the summary of crystallographic data are shown in Figure 1 and Table 1, respectively. The asymmetric unit of the monoclinic *P*₂₁/*n* crystal of *trans*-NO₂ contained one cationic ruthenium complex, one PF₆ anion, and one acetonitrile molecule. The *cis*-NO₂' crystallised with two crystallographically independent

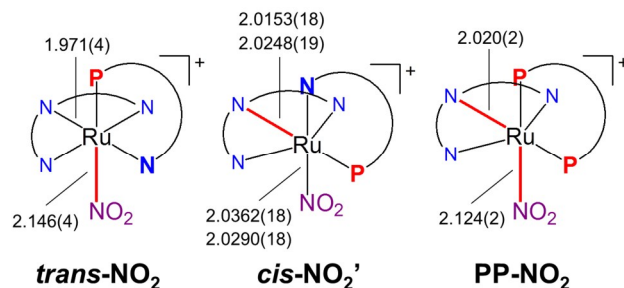


Figure 2 Comparison of bond distances (Å) around the ruthenium centres of *trans*-NO₂, *cis*-NO₂', and PP-NO₂.

ruthenium complexes, two BPh₄[−] anions, and one acetonitrile molecule as the crystal solvent in the asymmetric unit of the triclinic *P**T* space group. The asymmetric unit of the monoclinic *P*₂₁/*c* crystal of PP-NO₂ contained one cationic ruthenium complex, one PF₆ anion, and two methanol molecules. For each complex, the ratio of ruthenium to counter anion indicated that the oxidation state of the ruthenium centre was +2. The coordination geometry of each Ru atom was that of a distorted octahedron composed of a meridionally coordinated terpyridine ligand, a bidentate ligand, and a nitrito ligand.

The bond distances between the ruthenium and nitrogen atoms of the nitrito ligand of *trans*-NO₂ and PP-NO₂ were 2.146(4) (Ru1–N5) and 2.124(2) Å (Ru1–N4), respectively (Figure 2), and were longer than those found in [Ru(trpy)(bpm)(NO₂)]PF₆ (2.034(5) Å, bpm = 2, 2'-bipyrimidine).²⁵ By contrast, the Ru–N(NO₂) distances in *cis*-NO₂' (2.0362(18) and 2.0290(18) Å for Ru1–N5 and Ru2–N10, respectively, Figure 2) were similar to those of [Ru(trpy)(bpm)(NO₂)]PF₆ (2.034(5) Å). These results indicated a stronger *trans* influence of the phosphorous atom of Pqn or dpbz compared with that of the nitrogen atom of bpm or bpy. This tendency was also observed in *trans*-MeCN, *cis*-MeCN, and PP-MeCN in our previous study.²¹

UV-Vis Absorption Spectra

Figure 3 shows the UV-Vis absorption spectra of the nitrito-κ*N*

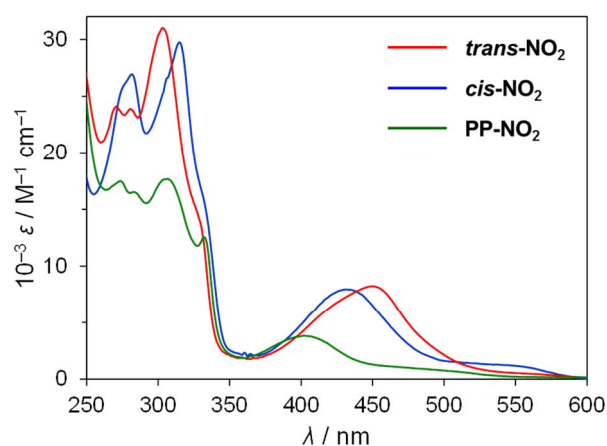


Figure 3 UV-Vis absorption spectra of *trans*-NO₂, *cis*-NO₂, and PP-NO₂ in acetonitrile at room temperature.

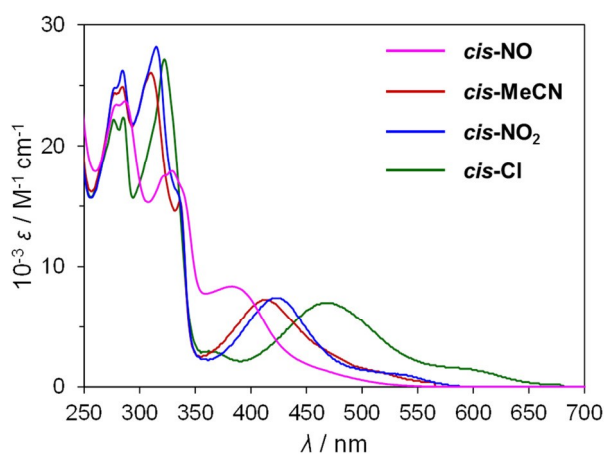


Figure 4 UV-Vis absorption spectra of $cis(P,X)-[Ru(trpy)(Pqn)(L)]^n$ ($L = Cl^-$, NO_2^- , $MeCN$, NO^+) in ethylene glycol at room temperature.

complexes, **trans-NO₂**, **cis-NO₂**, and **PP-NO₂**, in acetonitrile solution. The spectral data for these complexes and related compounds are listed in Table 2. All complexes displayed intense absorption bands in the UV region that were assigned to ligand-based $\pi-\pi^*$ transitions. Additionally, a moderately intense band was observed in the visible region for each complex. TD-DFT calculations that were performed at the B3LYP/LANL2DZ and B3LYP/SDD level of theory indicated that the visible region band could be assigned to metal-to-ligand charge transfer (MLCT) transitions from the $d\pi$ orbitals of ruthenium to the π^* orbitals of trpy and Pqn or dppbz (for details, see Table S1 and Figures S5-9 in the ESI). The molar absorption coefficient of **PP-NO₂** was nearly half those of **trans-NO₂** and **cis-NO₂**. The absorption maximum (λ_{max}) of the MLCT transition of **trans-NO₂**, **cis-NO₂**, and **PP-NO₂** was 443, 431, and 402 nm, respectively, and was blue-shifted compared with that of $[Ru(trpy)(bpm)(NO_2)]PF_6$,²⁵ suggesting the stabilisation of the $d\pi$ orbitals of the ruthenium centre upon introduction of the phosphine donors. Note that the MLCT band of **cis-NO₂** was more blue-shifted than that of **trans-NO₂** despite their isomeric relationship. A similar pattern was noted for the acetonitrile complexes, **trans-MeCN**, **cis-MeCN**, and **PP-MeCN**.²¹

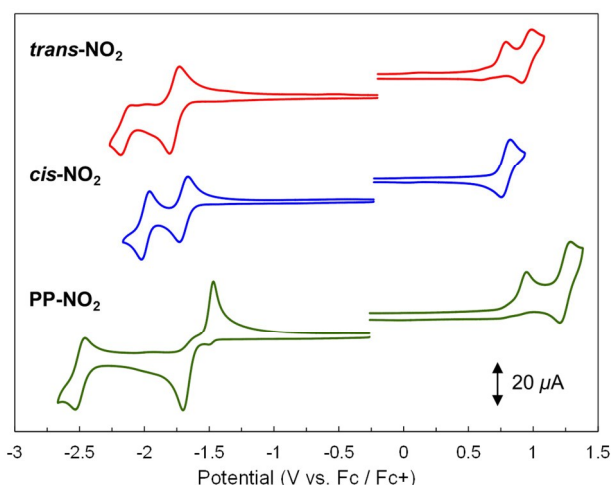


Figure 5 Cyclic voltammograms of **trans-NO₂**, **cis-NO₂**, and **PP-NO₂** (0.5 mM) in 0.1 M TEAP/acetonitrile under Ar atmosphere (WE: GC, CE: Pt wire, RE: Ag/Ag⁺; Scan rate: 100 mV/s).

The UV-vis absorption spectra of the *cis*-isomers with different ligands L , $cis(P,L)-[Ru(trpy)(Pqn)(L)]^{n+}$ ($L = Cl^-$, NO_2^- , $MeCN$, and NO^+), in ethylene glycol solution are shown in Figure 4. These complexes each exhibited ligand-based $\pi-\pi^*$ transitions in the UV region and MLCT transitions in the visible region. The MLCT transition of **cis-NO** was observed at $\lambda_{max} = 383$ nm and is comparable to similar Ru-NO complexes (Table 3). For the different L s, the lowest energy MLCT bands of the *cis*-isomers are in the following order: $L = Cl^-$ (468 nm) < NO_2^- (423 nm) < $MeCN$ (413 nm) < NO^+ (383 nm). This result can be attributed to the competing σ -donor/ π -acceptor properties of the respective ligands.

Electrochemical Properties

The cyclic voltammograms (CVs) of **trans-NO₂**, **cis-NO₂**, and **PP-NO₂** are shown in Figure 5, and electrochemical data for these complexes and related compounds are listed in Table 4. The CVs were measured in 0.1 M tetraethylammonium perchlorate (TEAP)/acetonitrile. **cis-NO₂** displayed one reversible oxidation wave in the positive region at $E_{1/2} = 0.79$ V vs. ferrocene/ferrocenium (Fc/Fc^+), which was assigned to a Ru(III)/Ru(II) redox couple. By contrast, **trans-NO₂** and **PP-**

Table 2 UV-Vis absorption data (λ_{max}/nm ($10^{-3} \epsilon/M^{-1} cm^{-1}$)) in acetonitrile and infrared data (ν/cm^{-1}) for **trans-NO₂**, **cis-NO₂**, **PP-NO₂**, and related compounds at room temperature.

complex	λ_{max}	IR	
		$\nu_{as}(NO_2)$	$\nu_s(NO_2)$
trans-NO₂	443 (8.02), 327 ^c , 303 (31.0), 281 (23.9), 271 (24.1)	1349	1304
cis-NO₂	431 (7.95), 331 ^c , 315 (29.7), 282 (26.9), 276 ^c	1339	1286
PP-NO₂	402 (3.82), 332 (12.6), 307 (17.7), 283 (16.5), 273 (17.5)	1354	1311
$[Ru(trpy)(bpy)(NO_2)]PF_6^a$	472	^d	^d
$[Ru(trpy)(bpm)(NO_2)]PF_6^b$	470 (6.50), 362 (6.10), 330 ^c , 308 (25.6), 264 (23.3)	1342	1286

[a] Reference 26. [b] Reference 25. [c] Absorption shoulder. [d] Data not collected.

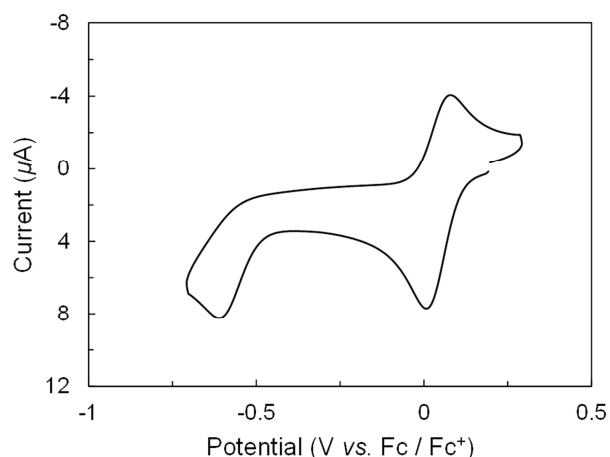


Figure 6 Cyclic voltammogram of *cis*-NO (0.5 mM) in 0.1 M TEAP/γ-butyrolactone under an Ar atmosphere (WE: GC, CE: Pt wire, RE: Ag/Ag⁺; Scan rate: 100 mV/s).

NO₂ exhibited one irreversible ($E_{pa} = 0.79$ for *trans*-NO₂ and 0.95 V for *PP*-NO₂) and one reversible ($E_{1/2} = 0.97$ for *trans*-NO₂ and 1.27 V for *PP*-NO₂) redox waves in the positive region. The former irreversible oxidation peak can be attributed to oxidation of the (Ru-NO₂)⁺ centre, and the latter reversible wave was observed exactly at the same potential as the Ru(III)/Ru(II) redox couple of the corresponding acetonitrile complex ($E_{1/2} = 0.97$ for *trans*-MeCN and 1.27 V for *PP*-MeCN, Table 4 and Figures S10b and 10d in the ESI).²¹ These observations suggest that the one-electron oxidation of *trans*-NO₂ and *PP*-NO₂ results in the release of NO₂, owing to the labilising effect of the *trans*-phosphine in each case. This leads to the formation of the respective ruthenium(II) acetonitrile complexes, which are oxidised reversibly on further sweep to more positive potential (Scheme 3). In the absence of a *trans*-labilising phosphine, the oxidation of the (Ru-NO₂)⁺ centre of *cis*-NO₂ occurs at a similar potential to the *trans*-isomer, but reversibly (Figure 5 and Table 4).

In the negative potential region, *cis*-NO₂ displayed two reversible reduction waves at -1.70 and -1.99 V, which were assigned to the trpy/trpy⁻ and Pqn/Pqn⁻ redox couple, respectively. *trans*-NO₂ exhibited two redox waves at $E_{1/2} = -1.77$ and -2.13 V, and these redox potentials were the same as that of *trans*-MeCN (Table 4 and Figure 10a in the ESI). *PP*-NO₂ displayed two irreversible waves ($E_{pc} = -1.70$ V and $E_{pa} =$

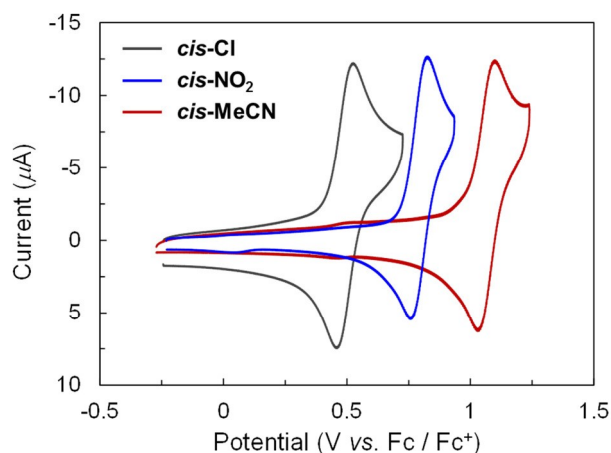


Figure 7 Cyclic voltammograms of *cis*-Cl, *cis*-NO₂, and *cis*-MeCN (0.5 mM) in 0.1 M TEAP/acetonitrile under an Ar atmosphere (WE: GC, CE: Pt wire, RE: Ag/Ag⁺; Scan rate: 100 mV/s).

-1.47 V) and one reversible ($E_{1/2} = -2.49$ V) redox wave in the negative region. The reversible wave at $E_{1/2} = -2.49$ V and the irreversible anodic wave at $E_{pa} = -1.47$ V were similar to those observed for *PP*-MeCN (Table 4 and Figure S10c in the ESI). These redox behaviours of *trans*-NO₂ and *PP*-NO₂ revealed that the reduction of these complexes induced the dissociation of NO₂⁻ and the formation of MeCN-coordinated species; this behaviour was similar to that observed in the positive potential region. The electrochemical behaviours of the nitrito-κN complexes are summarised in Scheme 3.

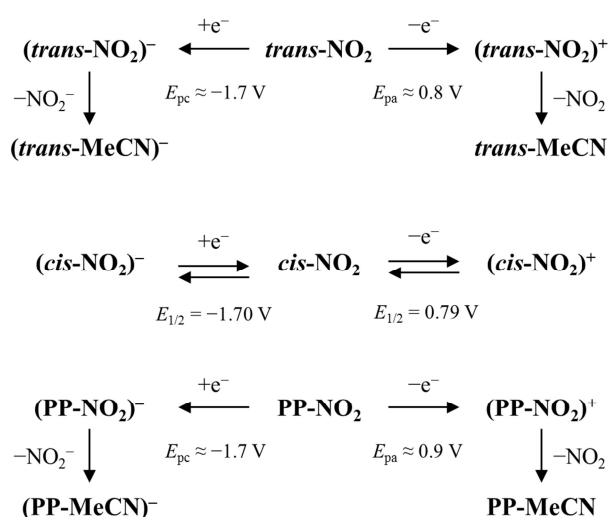
cis-NO displayed one reversible redox wave at $E_{1/2} = 0.05$ V and one irreversible reduction peak at $E_{pc} = -0.61$ V (Figure 6). Comparison with similar nitrosyl compounds^{24,25} revealed that the former redox wave was attributed to NO⁺/NO[•] redox couple and the latter peak could be assigned to the reduction of NO[•] to NO⁻. Note that a Ru(III)/Ru(II) redox couple was not observed in the potential region between -1.6 to 1.5 V due to the low HOMO energy level originating from the poor donating ability of the NO⁺ ligand.

Cyclic voltammograms of *cis*-isomers with various ligands L are shown in Figure 7. The redox potentials of a Ru(III)/Ru(II) redox couple for each complex were observed at 0.49, 0.79, and 1.05 V for *cis*(P,Cl)-[Ru(trpy)(Pqn)(Cl)]⁺ (*cis*-

Table 3 UV-Vis absorption data (λ_{max}/nm ($10^{-3} \text{ } \epsilon/M^{-1} \text{ cm}^{-1}$)) in acetonitrile, infrared data (ν/cm^{-1}), and redox potentials ($E_{1/2}/V$ vs Fc/Fc⁺) in acetonitrile for *cis*-NO and related compounds at room temperature.

complex	λ_{max}	ν_{N-O}	$E_{1/2}(\text{NO}^+/\text{NO}^\bullet)$	$E_{1/2}(\text{NO}^\bullet/\text{NO}^-)$
<i>cis</i> -NO ^a	383 (8.38), 329 (17.9), 323 ^d , 287 (23.7), 279 ^d	1929	0.05	-0.61 ^e
[Ru(trpy)(bpm)(NO)](PF ₆) ₃ ^b	362 (5.12), 331 ^d , 312 ^d , 291 (8.93), 265 (10.8)	1957	0.17	-0.47
<i>trans</i> (P,P)-[Ru(trpy)(PPh ₃) ₂ (NO)](ClO ₄) ₃ ^c	393 ^d , 330 (32)	1900	0.12	^f

[a] UV-Vis absorption data and redox potentials in ethylene glycol and γ-butyrolactone, respectively. [b] Reference 25. [c] Reference 24 [d] Absorption shoulder. [e] E_{pc} value for the irreversible process. [f] Data not collected.



Scheme 3 Electrochemical behaviour of nitrito-κN complexes.

Cl), *cis*-NO₂, and *cis*-MeCN, respectively. This result indicated the increase in the HOMO energy level by electron donation from monodentate ligands and was consistent with the UV-vis absorption spectroscopy.

Photostability of a Nitrosyl Complex

The photostability of *cis*-NO was investigated by UV-vis absorption spectroscopy and by using a Sievers nitric oxide analyser (NOA) to evaluate NO release. When a solution of *cis*-NO in ethylene glycol (0.05 mM) was irradiated at λ_{irr} = 355 nm, the slow spectral changes seen in Figure 8 were observed. The quantum yields of NO release, Φ_{NO}, were quite low, 0.0048 in air saturated solution and 0.003 under helium (ESI Figures S11-12). These Φ_{NO} values are about two orders of magnitude smaller than that measured by Silva et al. for the photolysis of the analogous ruthenium nitrosyl complex, [Ru(tpy)(bpy)(NO)]³⁺ (bpy = 2,2'-bipyridine).²⁷ Notably, exhaustive photolysis led to nearly quantitative conversion to a spectrum analogous to that of *trans*-L (L = solvent, see Figure

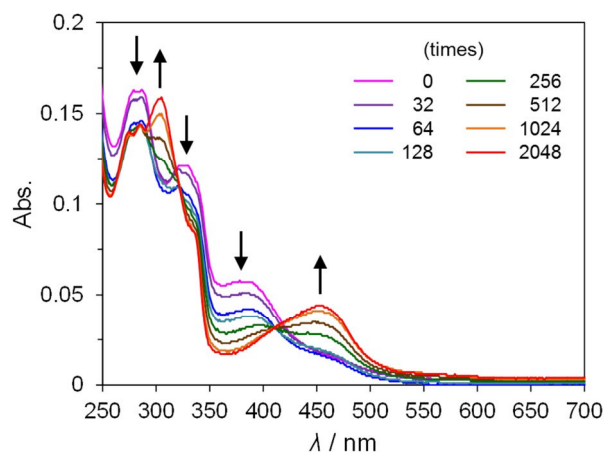


Figure 8 UV-Vis absorption spectra of *cis*-NO in ethylene glycol at room temperature during photolysis using a Nd/YAG laser operating at 355 nm. "Times" indicates the number of the laser pulses used to irradiate the sample.

S13 in the ESI), which suggests that the photodissociation of NO and the isomerization of the complex from *cis* to *trans* form proceeds in a step-wise manner. The result is consistent with the multi-step spectral change shown in Figure 8. It should further be noted that a Ru(II) complex, rather than the Ru(III) species is obtained upon NO photodissociation from *cis*-NO (ESI Figure S13). There are several possible explanations, one being that the Ru(III) intermediate is readily reduced by the solvent. Another is that the principal photo-reaction is release of NO⁺ rather than NO²⁷ owing to phosphine stabilization of the low-valent Ru(II) state. However, this question was not explored in greater detail.

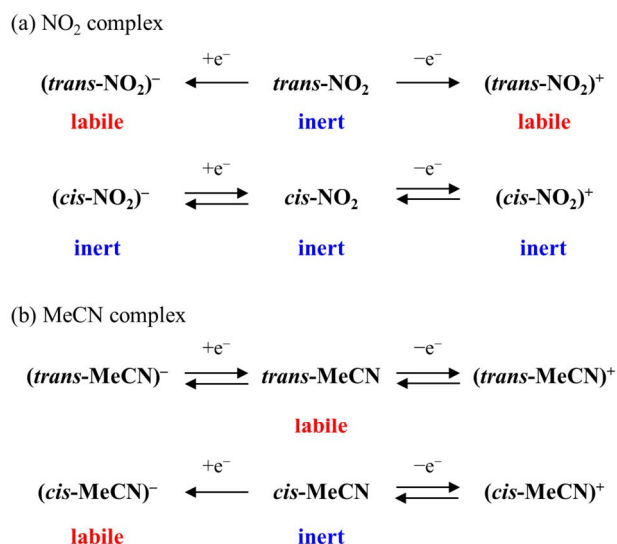
Substitution Lability of Nitrogen Oxide

The substitution lability of the monodentate ligand L in the [Ru(TL)(BL)(L)]ⁿ⁺-type complexes is an important factor in determining the reactivity of the complexes in various catalytic and photo-induced reactions. Several experimental results described above enabled us to discuss in detail the lability of the monodentate ligand in the complexes. First, the reaction of *cis*-NO₂ with HPF₆ afforded the desired *cis*-NO. However, the similar reactions of *trans*-NO₂ and PP-NO₂ resulted in the

Table 4. Redox potentials (V vs. Fc/Fc⁺) in acetonitrile for *trans*-NO₂, *cis*-NO₂, PP-NO₂, and related compounds at room temperature.

complex	Red.			Ox.	
	E(1)	E(2)	E(3)	E(1)	E(2)
<i>trans</i> -NO ₂	-1.77 ^b		-2.13 ^{c,g}	0.79 ^{c,f}	0.97 ^g
<i>cis</i> -NO ₂	-1.70	-1.99	-	0.79	-
PP-NO ₂	-1.70 ^{b,e}		-2.49 ^g	0.95 ^{c,f}	1.27 ^g
<i>trans</i> -MeCN ^a	-1.70	-1.77	-2.13	0.97	-
<i>cis</i> -MeCN ^a	^d	^d	^d	1.05	-
PP-MeCN ^a	-1.50	-1.46	-2.49	1.27	-

[a] Reference 21. [b] These reductions induced the dissociation of NO₂⁻ and the formation of MeCN-coordinated species. [c] NO₂ was released upon these oxidation processes, and subsequent coordination of MeCN resulted in the formation of corresponding acetonitrile complexes. [d] *cis*-MeCN underwent isomerization to *trans*-MeCN upon reduction. [e] E_{pc} values for the irreversible processes. [f] E_{pa} values for the irreversible processes. [g] Redox processes correspond to MeCN-coordinated complexes.



Scheme 4 Changes in lability with oxidation or reduction

formation of *trans*-MeCN and *PP*-MeCN via the dissociation *cis*-NO₂ with HPF₆ afforded the desired *cis*-NO. However, the similar reactions of *trans*-NO₂ and *PP*-NO₂ resulted in the formation of *trans*-MeCN and *PP*-MeCN via the dissociation of a monodentate labile ligand, N(O)OH or NO⁺ (probably the former). Second, UV-vis absorption spectroscopy revealed that the nitrito ligands of *trans*-NO₂, *cis*-NO₂, and *PP*-NO₂ did not dissociate, even in strongly coordinating solvents such as acetonitrile, whereas ligand exchange reactions of *trans*-MeCN and *PP*-MeCN easily occurred under analogous conditions (Figure S14 in the ESI). *cis*-NO was not stable in coordinating solvent and was easily converted to a solvent-coordinated form (Figure S4 in the ESI).

The difference in lability of the oxidised and reduced state can also be clarified by the results of the electrochemical measurements. In the one-electron oxidised states, *trans*-NO₂ and *PP*-NO₂ were labile and were converted to the solvent-coordinated forms, *trans*-MeCN and *PP*-MeCN, respectively. By contrast, *cis*-NO₂ was inert during the oxidation process, and a reversible redox wave was observed in the electrochemical measurement. Similarly, in the reduced states, the nitrito ligands of *trans*-NO₂ and *PP*-NO₂ easily dissociated, although *cis*-NO₂ was stable during the whole electrochemical process. However, this stability of *cis*-NO₂ was quite different from that of *cis*-MeCN: the acetonitrile ligand of *cis*-MeCN became labile upon reduction, and the dissociation of the ligand resulted in the isomerisation of *cis*-MeCN to *trans*-MeCN.²¹ The stability of the monodentate labile site for each complex is shown in Scheme 4.

The difference in the lability of these complexes can be explained by considering the following factors. First, the σ-donor character of phosphine group significantly elongates the bond length between the ruthenium centre and the ligand *trans* to the phosphine group. This *trans* influence of the phosphine group was clearly observed in the X-ray structure for the series

of nitrito-κN complexes; the bond distances between the ruthenium and nitrogen atom of the nitrite ligand are 2.141(3), 2.124 (2), and ca. 2.03 Å for *trans*-NO₂, *PP*-NO₂, and *cis*-NO₂, respectively. Therefore, the *trans*-isomers and *PP* complexes exhibited greater lability compared with the corresponding *cis*-isomers. Second, the electron donation from labile ligands can stabilise Ru-L bonds. The donating ability of labile ligands was confirmed by the comparison of the HOMO energy levels obtained from the electrochemical measurements of the *cis*-isomers and follows the order NO₂⁻ > MeCN > NO⁺ and was in accordance with the stability of the complexes. Third, oxidation decreases the electron density of the Ru centre, and the π back-donating ability of Ru centres should be weakened. DFT calculations revealed that π back-donation from Ru to the nitrito ligand occurs and stabilises the Ru-L bond (Figure S6 in the ESI). Finally, the reduction of the complexes stabilises the five-coordinated species, as rationalised for the Ru(II)-MeCN complexes in our previous report.²¹ The formation of five-coordinated species in MeCN results in ligand exchange in *trans*-NO₂ and *PP*-NO₂ or isomerisation of *cis*-MeCN to *trans*-MeCN, whereas no observable chemical process exists in the case of *cis*-NO₂, *trans*-MeCN and *PP*-MeCN. These results suggest that the (1) number and position of P atom(s), (2) coordinating ability of the monodentate ligand, and (3) oxidation state of the complexes are all factors in defining the lability of complexes.

Conclusions

This study describes the syntheses, crystal structures and spectroscopic and electrochemical properties of a series of phosphine-substituted ruthenium(II) polypyridine complexes with nitrogen oxides. Three nitrito-κN complexes, *trans*-NO₂, *cis*-NO₂, and *PP*-NO₂ were synthesised by the reaction of the corresponding acetonitrile complex with NaNO₂ in an ethanol/water mixed solution, and a nitrosyl complex, *cis*-NO, was obtained by the reaction of *cis*-NO₂ with HPF₆ in acetone. Crystallographic, spectroscopic, and electrochemical analyses for these complexes revealed that the σ-donating and π-accepting characters of the phosphine ligands clearly affected the dσ and dπ orbitals of the ruthenium centre, respectively. The investigation of the substitution lability of the monodentate ligand of each complex suggested that the (1) number and position of the phosphine groups, (2) coordinating ability of monodentate ligand, and (3) oxidation state of the metal centre are all factors in determining the lability of the complex. As a further extension of our studies, investigations on various catalytic and photo-induced reactions of the phosphine-substituted ruthenium(II) polypyridine complexes are in progress in our laboratories.

Experimental

Materials

NaNO₂ was purchased from Kanto Chemical Co., Inc. NH₄PF₆ and HPF₆ were purchased from Wako Pure Chemical Industries, Ltd. All solvents and reagents were of the highest quality available and were used as received. *trans*(*P*,*MeCN*)- and *cis*(*P*,*MeCN*)-[Ru(*trpy*)(*Pqn*)(*MeCN*)](PF₆)₂ (**trans-MeCN** and **cis-MeCN**), and [Ru(*trpy*)(*dppbz*)(*MeCN*)](PF₆)₂ (**PP-MeCN**) were prepared following methods found in the literature.¹⁸

Measurements

¹H and ³¹P{¹H} NMR spectra were recorded at room temperature on a JEOL JNM-LA500 spectrometer using tetramethylsilane as an internal reference for the ¹H NMR spectra and phosphoric acid as an external reference for the ³¹P{¹H} NMR spectra. UV-vis absorption spectra were obtained on a Shimadzu UV-2450SIM spectrophotometer at room temperature. Elemental analyses were carried out on a Yanagimoto MT-5 elemental analyser. Infrared data were obtained using a Perkin-Elmer Spectrum 100 FT-IR spectrometer. ESI-TOF mass spectra were recorded on a JEOL JMS-T100LC mass spectrometer. All the ESI-TOF mass spectrometric measurements were recorded in the positive ion mode at a cone voltage of 20 V. Typically, each sample solution was introduced in the spectrometer at a flow rate of 10 mL/min using a syringe pump. Cyclic voltammograms were measured at room temperature on a BAS ALS Model 650DKMP electrochemical analyser in acetonitrile ([complex] = 0.5 mM; 0.1 M tetraethylammonium perchlorate (TEAP)). A glassy carbon disk, platinum wire, and Ag/Ag⁺ electrode (Ag / 0.01 M AgNO₃) were used as the working, auxiliary, and reference electrodes, respectively. The redox potentials of the samples were calibrated against the redox signal for the ferrocene/ferrocenium (Fc/Fc⁺) couple. The photochemical experiments shown in Figure 8 were made using a photolysis apparatus consisting of a LS-2134UTF Nd/YAG laser (Tokyo Instruments, INC.) with excitation provided by the third harmonic at λ = 355 nm. The pulse width was 5 ns, the beam diameter incident on the sample was 6 mm, and the repetition rate was 5 Hz.

Synthetic procedures

Synthesis of *trans*(*P*,*NO*₂)-[Ru(*trpy*)(*Pqn*)(*NO*₂)]PF₆ (trans-NO**₂).** A mixture of **trans-MeCN** (26.8 mg, 0.0252 mmol) and NaNO₂ (38.8 mg, 0.562 mmol) in ethanol (4 cm³)/water (4 cm³) was heated at 100°C for 3 hours and then cooled to room temperature. Acetonitrile (2 cm³) and a NH₄PF₆ (188.4 mg, 1.16 mmol)/water (2 cm³) solution was added to the abovementioned solution. The resulting red solution was concentrated to ca. 5 cm³ under reduced pressure. The red product was collected by filtration and washed with water and diethyl ether. Yield 19.1 mg (0.0216 mmol, 86%). Single red crystals suitable for X-ray crystallography were grown by the slow diffusion of diethyl ether into a mixture of methanol and a few drops of acetonitrile solution of **trans-NO**₂. ESI-TOF MS (positive ion, acetonitrile): *m/z* 694 ([Ru(*trpy*)(*Pqn*)(*NO*₂)]⁺). ¹H

NMR (CD₃CN): δ 6.56 (t, 2H, *J* = 9.0 Hz), 6.98 (t, 4H, *J* = 7.0 Hz), 7.14 (t, 2H, *J* = 7.0 Hz), 7.21 (t, 2H, *J* = 8.0 Hz), 7.65 (d, 2H, *J* = 5.0 Hz), 7.80 (t, 2H, *J* = 8.0 Hz), 7.91 (m, 3H), 8.03 (d, 2H, *J* = 8.0 Hz), 8.09 (t, 1H, *J* = 7.5 Hz), 8.23 (d, 2H, *J* = 8.0 Hz), 8.46 (d, 1H, *J* = 7.0 Hz), 8.75 (d, 1H, *J* = 8.0 Hz), 9.93 (d, 1H, *J* = 5.0 Hz). ³¹P{¹H} NMR (CD₃CN): δ 53.10 (s). FT-IR: ν_s(NO₂) 1304, ν_{as}(NO₂) 1349 cm⁻¹. Anal. Found: C, 48.50; H, 3.59; N, 8.22. Calcd for C₃₆H₃₂F₆N₅O_{4.5}P₂Ru (**trans-NO**₂·2.5H₂O): C, 48.93; H, 3.65; N, 7.93.

Synthesis of *cis*(*P*,*NO*₂)-[Ru(*trpy*)(*Pqn*)(*NO*₂)]PF₆ (cis-NO**₂).** This complex was prepared from **cis-MeCN** (26.0 mg, 0.0250 mmol) instead of **trans-MeCN** by a method similar to that for **trans-NO**₂. Yield 19.5 mg (0.0221 mmol, 88%). ESI-TOF MS (positive ion, acetonitrile): *m/z* 694 ([Ru(*trpy*)(*Pqn*)(*NO*₂)]⁺). ¹H NMR (CD₃CN): δ 6.81 (t, 2H, *J* = 6.5 Hz), 7.06 (m, 1H), 7.41 (d, 2H, *J* = 5.5 Hz), 7.52 (m, 4H), 7.63 (t, 2H, *J* = 7.5 Hz), 7.73 (m, 4H), 7.84 (t, 2H, *J* = 8.0 Hz), 7.92 (d, 1H, *J* = 5.5 Hz), 7.97 (t, 1H, *J* = 7.5 Hz), 8.18 (d, 1H, *J* = 8.0 Hz), 8.23 (d, 1H, *J* = 8.0 Hz), 8.36 (m, 3H), 8.55 (d, 2H, *J* = 8.0 Hz), 8.78 (t, 1H, *J* = 8.0 Hz). ³¹P{¹H} NMR (CD₃CN): δ 54.06 (s). FT-IR: ν_s(NO₂) 1286, ν_{as}(NO₂) 1339 cm⁻¹. Anal. Found: C, 50.38; H, 3.44; N, 8.19. Calcd for C₃₆H₂₉F₆N₅O₃P₂Ru (**cis-NO**₂·H₂O): C, 50.47; H, 3.41; N, 8.18.

Synthesis of *cis*(*P*,*NO*₂)-[Ru(*trpy*)(*Pqn*)(*NO*₂)]BPh₄ (cis-NO**₂’).** This complex was prepared by a method similar to that for **cis-NO**₂ with an excess of NaBPh₄ instead of NH₄PF₆. The product was recrystallised from dichloromethane and a small amount of acetonitrile/diethyl ether to afford orange-red crystals of **cis-NO**₂’. Anal. Found: C, 70.54; H, 4.72; N, 6.92. Calcd for C₆₀H₄₈BN₅O_{2.5}PRu (**cis-NO**₂’·0.5H₂O): C, 70.52; H, 4.73; N, 6.85.

Synthesis of *cis*(*P*,*NO*)-[Ru(*trpy*)(*Pqn*)(*NO*)](PF₆)₃ (cis-NO**).** **cis-NO**₂ (22.4 mg, 0.0261 mmol) was dissolved in acetone (1 cm³). An excess of 60% HPF₆ acid solution was added dropwise until the solution changed colour from red to yellow in an ice-water bath. The resulting yellow solution was concentrated under reduced pressure, and 10 cm³ of diethyl ether was added to precipitate the product. Yield 27.4 mg (0.0223 mmol, 85%). ¹H NMR (acetone-*d*₆): δ 7.47 (t, 2H, *J* = 7.0 Hz), 7.66 (m, 1H), 7.80 (d, 2H, *J* = 6.0 Hz), 7.86 (m, 4H), 8.01 (t, 2H, *J* = 7.5 Hz), 8.12 (dd, 4H, *J* = 7.5, 13.0 Hz), 8.42 (t, 1H, *J* = 7.5 Hz), 8.49 (m, 2H), 8.55 (m, 1H), 8.80 (d, 1H, *J* = 8.0 Hz), 9.01 (m, 3H), 9.10 (m, 1H), 9.22 (m, 3H). ³¹P{¹H} NMR (acetone-*d*₆): δ 54.23 (s). FT-IR: ν_s(NO) 1929 cm⁻¹. Anal. Found: C, 35.03; H, 2.95; N, 5.59. Calcd for C₃₆H₄₀F₁₈N₅O_{7.5}P₄Ru (**cis-NO**·6.5H₂O): C, 35.16; H, 3.28; N, 5.70.

Synthesis of [Ru(*trpy*)(*dppbz*)(*NO*₂)]PF₆ (PP-NO**₂).** This complex was prepared from **PP-MeCN** (31.5 mg, 0.0263 mmol) instead of **trans-MeCN** by a method similar to that for **trans-NO**₂. Yield 22.9 mg (0.0227 mmol, 86%). Single orange crystals suitable for X-ray crystallography were grown through the slow diffusion of diethyl ether into a mixture of methanol and a few drops of acetonitrile solution of **PP-NO**₂. ESI-TOF MS (positive ion, acetonitrile): *m/z* 827 ([Ru(*trpy*)(*dppbz*)(*NO*₂)]⁺). ¹H NMR (CD₃CN): δ 6.50 (m, 4H),

6.78 (m, 2H), 6.88 (m, 4H), 7.08 (d, 2H, $J = 5.5$ Hz), 7.17 (m, 2H), 7.45 (t, 4H, $J = 7.5$ Hz), 7.61 (m, 7H), 7.77 (m, 3H), 7.87 (t, 1H, $J = 7.5$ Hz), 8.03 (d, 2H, $J = 8.0$ Hz), 8.23 (m, 3H), 8.39 (t, 1H, $J = 7.5$ Hz). $^{31}\text{P}\{^1\text{H}\}$ NMR (CD_3CN): δ 62.65 (d, $^2J_{\text{P-P}} = 14.2$ Hz), 68.59 (d, $^2J_{\text{P-P}} = 14.2$ Hz). FT-IR: $\nu_{\text{s}}(\text{NO}_2)$ 1311, $\nu_{\text{as}}(\text{NO}_2)$ 1354 cm^{-1} . Anal. Found: C, 53.62; H, 4.05; N, 5.46. Calcd for $\text{C}_{45}\text{H}_{39}\text{F}_6\text{N}_4\text{O}_4\text{P}_3\text{Ru}$ (**PP-NO₂**·2H₂O): C, 53.63; H, 3.90; N, 5.56.

X-ray crystallography

The X-ray data collection and processing was performed on a Kappa APEX II CCD diffractometer by using graphite-monochromated Mo-K α radiation (0.71075 Å) for **trans-NO₂** and **PP-NO₂**. Single-crystal X-ray diffraction measurement of **cis-NO₂** was performed with a RAXIS-RAPID Imaging Plate diffractometer equipped with confocal monochromated Mo-K α (0.71075 Å) radiation, and the data were processed using RAPID-AUTO (Rigaku). The structure was solved by the direct method using SIR-92²⁸ and refined on F^2 with the full-matrix least squares technique using SHELXL-2014.²⁹ All non-hydrogen atoms were refined anisotropically. Molecular graphics were generated using ORTEP-3 for Windows³⁰ and POV-RAY.³¹ A summary of the crystallographic data and structure refinement parameters is given in Table 1.

The crystallographic data have been deposited at the Cambridge Crystallographic Data Centre: Deposition numbers CCDC 1040452, 1040453, and 1040454 for **trans-NO₂**, **cis-NO₂**, and **PP-NO₂**, respectively. Copies of the data can be obtained free of charge via www.ccdc.cam.ac.uk/data_request/cif.

DFT calculations

Calculations were performed using the DFT method implemented in the Gaussian 09 package.³² The structures were fully optimised using the hybrid B3LYP method, which uses Becke's three-parameter exchange functional³³ with the correlation energy functional of Lee, Yang, and Parr.³⁴ All calculations were performed using the standard double- ζ type LANL2DZ basis set^{35a-c} or SDD basis set^{35d} implemented in Gaussian 09, without adding any extra polarisation or diffuse functions. The LANL2DZ basis set also uses a relativistic effective core potential (RECP) for the Ru atom to account for the scalar relativistic effects of the inner 28 core electrons ([Ar]3d¹⁰). All calculations were performed using the polarisable continuum model (PCM)³⁶ to compute the structures in acetonitrile media. All stationary points were characterised as minima of the potential energy surface by their harmonic vibrational frequencies. The free energies at 298 K and 1 atm were obtained through thermochemical analysis of the frequency calculation using the thermal correction to Gibbs free energy as implemented in Gaussian 09. The excited states were calculated using the TDDFT³⁷ method within the Tamm-Dancoff approximation as implemented in Gaussian 09. These calculations employ the hybrid B3LYP functional along with the basis sets described above. A minimum of 100 excited states was computed in each calculation. To obtain the

simulated spectrum of each species, transition energies and oscillator strengths were interpolated by a Gaussian convolution with a common σ value of 0.2 eV.

Quantum Yield Measurements

Nitric oxide was detected and analysed using a GE Sievers model 280i nitric oxide analyser (NOA).³⁸ Known volumes of the gases from the solution headspace were injected into the NOA purge vessel, and these gases were entrained to the detector using helium or medical grade air. The NO present in the sample was quantified using a calibration curve generated from the reaction of NaNO₂ with acidic KI. Chemical actinometry was performed with ferric oxalate solutions.³⁹ The photolysis source was the output from a 200 W high-pressure mercury lamp passed through an IR filter and collimated with lenses. An appropriate interference filter was used to select the desired λ_{irr} . A shutter shielded the sample from the arc lamp. A sample of known volume in a 1 cm square cuvette with a magnetic stirring bar was irradiated for determined time periods.⁴⁰ The NO quantum yields (Φ_{NO}) were calculated based on the nitric oxide release measured using the NOA.

Acknowledgements

This work was supported by a Grant-in-Aid for Young Scientists (A) (No. 25708011) (to S.M.), a Grant-in-Aid for Challenging Exploratory Research (No. 26620160) (to S.M.), and a Grant-in-Aid for Young Scientists (B) (No. 24750140) (to M.K.) from the Japan Society for the Promotion of Science. This work was also supported by a Grant-in-Aid for Scientific Research on Innovative Areas "AnApple" (No. 25107526). Studies at UCSB were supported by a US National Foundation Grant (CHE-1058794 and CHE-1405062). We thank Dr. Guang Wu of UCSB for the X-ray diffraction studies and Dr. John Garcia of UCSB for confirming photochemical results.

Notes and references

^a Institute for Molecular Science (IMS), 5-1 Higashiyama, Myodaiji, Okazaki, Aichi 444-8787, Japan. E-mail: masaoka@ims.ac.jp; Fax: +81-564-59-5589

^b Department of Structural Molecular Science, School of Physical Sciences, SOKENDAI (The Graduate University for Advanced Studies), Shonan Village, Hayama-cho, Kanagawa 240-0193, Japan.

^c ACT-C, Japan Science and Technology Agency (JST), 4-1-8 Honcho, Kawaguchi, Saitama, 332-0012, Japan.

^d Research Center of Integrative Molecular Systems (CIMoS), Institute for Molecular Science, 38 Nishigo-naka, Myodaiji, Okazaki, Aichi 444-8585, Japan.

^e Department of Chemistry and Biochemistry, University of California at Santa Barbara, Santa Barbara, California 93106-9510, United States

† Electronic Supplementary Information (ESI) available: [details of any supplementary information available should be included here]. See DOI: 10.1039/b000000x/

- (a) N. Sutin, *J. Photochem.*, 1979, **10**, 19–40; (b) K. Kalyanasundaram, *Coord. Chem. Rev.*, 1982, **46**, 159–244; (c) E. S. Dodsworth, A. B. P. Lever, *Chem. Phys. Lett.*, 1986, **124**, 152–158; (d) A. Juris, V. Balzani, F. Barigelli, S. Campagna, P. Belser, A.

- von Zelewsky, *Coord. Chem. Rev.*, 1988, **84**, 85–277; (e) A. B. P. Lever, *Inorg. Chem.*, 1990, **29**, 1271–1285; (f) V. Balzani, A. Juris, *Coord. Chem. Rev.*, 2001, **211**, 97–115; (g) D. W. Thompson, J. F. Wishart, B. S. Brunswig, N. Sutin, *J. Phys. Chem. A*, 2001, **105**, 8117–8122. (h) S. Campagna, F. Puntoriero, F. Nastasi, G. Bergamini, V. Balzani, *Top. Curr. Chem.*, 2007, **280**, 117–214; (i) T. P. Yoon, M. A. Ischay, J. Du, *Nat. Chem.*, 2010, **2**, 527–532; (j) Q. Sun, S. Mosquera-Vazquez, Y. Suffren, J. Hankache, N. Amstutz, L. M. L. Daku, E. Vauthey, A. Hauser, *Coord. Chem. Rev.*, 2015, **282–283**, 87–99.
2. (a) C. D. Clark, M. Z. Hoffman, *Coord. Chem. Rev.*, 1997, **159**, 359–373; (b) L. De Cola, P. Belser, *Coord. Chem. Rev.*, 1998, **177**, 301–346; (c) M. D. Ward, F. Barigelletti, *Coord. Chem. Rev.*, 2001, **216–217**, 127–154; (d) M. H. V. Huynh, D. M. Dattelbaum, T. J. Meyer, *Coord. Chem. Rev.*, 2005, **249**, 457–483. (d) H. Kon, K. Tsuge, T. Imamura, Y. Sasaki, S. Ishizaka, N. Kitamura, M. Kato, *Dalton Trans.*, 2008, 1541–1543; (e) A. Lavie-Cambot, C. Lincheneau, M. Cantuel, Y. Leydet, N. D. McClenaghan, *Chem. Soc. Rev.*, 2010, **39**, 506–515; (f) O. Filevich, B. Garcia-Acosta, R. Etchenique, *Photochem. Photobiol. Sci.*, 2012, **11**, 843–847.
 3. (a) F. G. Gao, A. J. Bard, *J. Am. Chem. Soc.*, 2000, **122**, 7426–7427; (b) J. N. Demas, B. A. DeGraff, *Coord. Chem. Rev.*, 2001, **211**, 317–351; (c) P. D. Beer, E. J. Hayes, *Coord. Chem. Rev.*, 2003, **240**, 167–189; (d) R. Martinez-Mañez, F. Sancenón, *Chem. Rev.*, 2003, **103**, 4419–4476; (e) A. S. Polo, M. K. Itokazu, N. Y. M. Iha, *Coord. Chem. Rev.*, 2004, **248**, 1343–1361; (f) M. S. Vickers, K. S. Martindale, P. D. Beer, *J. Mater. Chem.*, 2005, **15**, 2784–2790; (g) N. Haddour, J. Chauvin, C. Gondran, S. Cosnier, *J. Am. Chem. Soc.*, 2006, **128**, 9693–9698; (h) H. Wei, E. Wang, *Trends Anal. Chem.*, 2008, **27**, 447–459; (i) J. L. Delaney, C. F. Hogan, J. Tian, W. Shen, *Anal. Chem.*, 2011, **83**, 1300–1306.
 4. (a) G. J. Wilson, A. Launikonis, W. H. F. Sasse, A. W.-H. Mau, *J. Phys. Chem. A*, 1997, **101**, 4860–4866; (b) J. A. Simon, S. L. Curry, R. H. Schmehl, T. R. Schatz, P. Piotrowiak, X. Jin, R. P. Thummel, *J. Am. Chem. Soc.*, 1997, **119**, 11012–11022; (c) A. D. Guerso, S. Leroy, F. Fages, R. H. Schmehl, *Inorg. Chem.*, 2002, **41**, 359–366; (d) D. S. Tyson, C. R. Luman, X. Zhou, F. N. Castellano, *Inorg. Chem.*, 2001, **40**, 4063–4071; (e) S. Bernhard, J. A. Barron, P. L. Houston, H. D. Abreuña, J. L. Ruglovksy, X. Gao, G. G. Malliaras, *J. Am. Chem. Soc.*, 2002, **128**, 9693–9698; (f) S. Welter, K. Brunner, J. W. Hofstra, L. D. Cola, *Nature*, 2003, **421**, 54–57; (g) H. Shahroosvand, P. Abbasi, A. Faghhi, E. Mohajerani, M. Janghour, M. Mahmoudi, *RSC Adv.*, 2014, **4**, 1150–1154.
 5. (a) J. K. Barton, *Science*, 1986, **233**, 727–734; (b) C. Turro, S. H. Bossmann, Y. Jenkins, J. K. Barton, N. J. Turro, *J. Am. Chem. Soc.*, 1995, **117**, 9026–9032; (c) H. B. Gray, J. R. Winkler, *Ann. Rev. Biochem.*, 1996, **65**, 537–561; (d) A. D. Guerso, A. K.-D. Mesmaeker, *Inorg. Chem.*, 2002, **41**, 938–945; (e) S. Le Gac, M. Foucart, P. Gerbaux, E. Defrancq, C. Moucheron, A. Kirsch-De Mesmaeker, *Dalton Trans.*, 2010, **39**, 9672–9683; (f) H. Song, J. T. Kaiser, J. K. Barton, *Nat. Chem.*, 2012, **4**, 615–620; (g) H. Niyazi, J. P. Hall, K. O'Sullivan, G. Winter, T. Sorensen, J. M. Kelly, C. J. Cardin, *Nat. Chem.*, 2012, **4**, 621–628; (h) A. C. Komor, J. K. Barton, *Chem. Commun.*, 2013, **49**, 3617–3630.
 6. (a) T. J. Meyer, M. H. V. Huynh, *Inorg. Chem.*, 2003, **42**, 8140–8160; (b) E. Masllorens, M. Rodriguez, I. Romero, A. Roglans, T. Parella, J. Benet-Buchholz, M. Poyatos, A. Llobet, *J. Am. Chem. Soc.*, 2006, **128**, 5306–5307; (c) Y. Shiota, J. M. Herrera, Gergely Juhász, T. Abe, S. Ohzu, T. Ishizuka, T. Kojima, K. Yoshizawa, *Inorg. Chem.*, 2011, **50**, 6200–6209; (d) T. Kojima, K. Nakayama, K. Ikemura, T. Ogura, S. Fukuzumi, *J. Am. Chem. Soc.*, 2011, **133**, 11692–11700; (e) Z. Hu, H. Du, W.-L. Man, C.-F. Leung, H. Liang, T.-C. Lau, *Chem. Commun.*, 2012, **48**, 1102–1104; (f) Z. Hu, L. Ma, J. Xie, H. Du, W. W. Y. Lam, T.-C. Lau, *New J. Chem.*, 2013, **37**, 1707–1710.
 7. (a) J. J. Concepcion, J. W. Jurss, J. L. Templeton, T. J. Meyer, *J. Am. Chem. Soc.*, 2008, **130**, 16462–16463; (b) H.-W. Tseng, R. Zong, J. T. Muckerman, R. P. Thummel, *Inorg. Chem.*, 2008, **47**, 11763–11773; (c) S. Masaoka, K. Sakai, *Chem. Lett.*, 2009, **38**, 182–183; (d) M. Yoshida, S. Masaoka, K. Sakai, *Chem. Lett.*, 2009, **38**, 702–703; (e) S. Romain, L. Vigara, A. Llobet, *Acc. Chem. Res.*, 2009, **42**, 1944–1953; (f) J. J. Concepcion, J. W. Jurss, M. K. Brennaman, P. G. Hoertz, A. O. T. Patrocinio, N. Y. Murakami Iha, J. L. Templeton, T. J. Meyer, *Acc. Chem. Res.*, 2009, **42**, 1954–1965; (g) L. Duan, L. Tong, Y. Xu, L. Sun, *Energy Environ. Sci.*, 2011, **4**, 3296–3313; (h) D. J. Wasylenko, R. D. Palmer, C. P. Berlinguette, *Chem. Commun.*, 2013, **49**, 218–227; (i) M. D. Kärkäs, O. Verho, E. V. Johnston, B. Åkermark, *Chem. Rev.*, 2014, **114**, 11863–12001.
 8. (a) H. Yamazaki, T. Hakamata, M. Komi, M. Yagi, *J. Am. Chem. Soc.*, 2011, **133**, 8846–8849; (b) J. L. Boyer, D. E. Polyansky, D. J. Szalda, R. Zong, R. P. Thummel, E. Fujita, *Angew. Chem. Int. Ed.*, 2011, **50**, 12600–12604; (c) S. K. Padhi, R. Fukuda, M. Ehara, K. Tanaka, *Inorg. Chem.*, 2012, **51**, 5386–5392; (d) M. Hirahara, M. Z. Ertem, M. Komi, H. Yamazaki, C. J. Cramer, M. Yagi, *Inorg. Chem.*, 2013, **52**, 6354–6364.
 9. (a) K. Tanaka, D. Ooyama, *Coord. Chem. Rev.*, 2002, **226**, 211–218; (b) J.-M. Savéant, *Chem. Rev.*, 2008, **108**, 2348–2378; (c) Y. Tsukahara, T. Wada, K. Tanaka, *Chem. Lett.*, 2010, **39**, 1134–1135; (d) K. Kobayashi, T. Kikuchi, S. Kitagawa, K. Tanaka, *Angew. Chem. Int. Ed.*, 2014, **52**, 1–6.
 10. (a) Z. Chen, C. Chen, D. R. Weinberg, P. Kang, J. J. Concepcion, D. P. Harrison, M. S. Brookhart, T. J. Meyer, *Chem. Commun.*, 2011, **47**, 12607–12609; (b) Z. Chen, J. J. Concepcion, M. K. Brennaman, P. Kang, M. R. Norris, P. G. Hoertz, T. J. Meyer, *Proc. Natl. Acad. Sci. USA*, 2012, **109**, 15606–15611; (c) Z. Chen, P. Kang, M.-T. Zhang, T. J. Meyer, *Chem. Commun.*, 2014, **50**, 335–337; (d) P. Kang, Z. Chen, A. Nayak, S. Zhang, T. J. Meyer, *Energy Environ. Sci.*, 2014, **7**, 4007–4012.
 11. (a) A. Kobayashi, R. Takatori, I. Kikuchi, H. Konno, K. Sakamoto, O. Ishitani, *Organometallics*, 2001, **20**, 3361–3363; (b) A. Kobayashi, H. Konno, K. Sakamoto, A. Sekine, Y. Ohashi, M. Iida, O. Ishitani, *Chem. Eur. J.*, 2005, **11**, 4219–4226; (c) M. Kimura, K. Tanaka, *Angew. Chem. Int. Ed.*, 2008, **47**, 9768–9771; (d) Y. Matsubara, E. Fujita, M. D. Doherty, J. T. Muckerman, C. Creutz, *J. Am. Chem. Soc.*, 2012, **134**, 15743–15757; (e) Y. Matsubara, T. Kosaka, K. Koga, A. Nagasawa, A. Kobayashi, H. Konno, C. Creutz, K. Sakamoto, O. Ishitani, *Organometallics*, 2013, **32**, 6162–6165; (f) J. Huang, J. Chen, H. Gao, L. Chen, *Inorg. Chem.*, 2014, **53**, 9570–9580.
 12. (a) R. W. Callahan, T. J. Meyer, *Inorg. Chem.*, 1977, 574–581; (b) H. Hadadzadeh, M. C. DeRosa, G. P. A. Yap, A. R. Rezvani, R. J. Crutchley, *Inorg. Chem.*, 2002, **41**, 6521–6526; (c) M. G. Sauaia, R.

- G. de Lima, A. C. Tedesco, R. S. da Silva, *J. Am. Chem. Soc.*, 2003, **125**, 14718–14719; (d) Z. N. da Rocha, M. S. P. Marchesi, J. C. Molin, C. N. Lunardi, K. M. Miranda, L. M. Bendhack, P. C. Ford, R. S. da Silva, *Dalton Trans.*, 2008, 4282–4287; (e) A. C. Pereira, P. C. Ford, R. S. da Silva, L. M. Bendhack, *Nitric Oxide*, 2011, **24**, 192–198; (f) T. A. Heinrich, A. C. Tedesco, J. M. Fukuto, R. S. da Silva, *Dalton Trans.*, 2014, **43**, 4021–4025; (g) R. G. de Lima, B. R. Silva, R. S. da Silva, L. M. Bendhack, *Molecules*, 2014, **19**, 9628–9654.
13. (a) T. Kinoshita, J. T. Dy, S. Uchida, T. Kubo, H. Segawa, *Nat. Photonics*, 2013, **7**, 535–539; (b) R. Katoh, A. Furube, *J. Photochem. Photobiol. C*, 2014, **20**, 1–16.
14. (a) R. Noyori, T. Ohkuma, *Angew. Chem. Int. Ed.*, 2001, **40**, 40–73; (b) R. Noyori, *Angew. Chem. Int. Ed.*, 2002, **41**, 2008–2022; (c) R. Noyori, *Adv. Synth. Catal.*, 2003, **345**, 15–32; (d) S. E. Clapham, A. Hadzovic, R. H. Morris, *Coord. Chem. Rev.*, 2004, **248**, 2201–2237; (e) A. F. Trindade, P. M. P. Gois, C. A. M. Afonso, *Chem. Rev.*, 2009, **109**, 418–514. (f) R. Noyori, *Angew. Chem. Int. Ed.*, 2013, **52**, 79–92.
15. (a) P. Schwab, M. B. France, J. W. Ziller, R. H. Grubbs, *Angew. Chem. Int. Ed.*, 1995, **34**, 2039–2041; (b) H. Clavier, S. P. Nolan, *Chem. Eur. J.*, 2007, **13**, 8029–8036; (c) G. C. Vougioukalakis, R. H. Grubbs, *Chem. Rev.*, 2010, **110**, 1746–1787; (d) J. S. M. Samec, B. K. Keitz, R. H. Grubbs, *J. Organomet. Chem.*, 2010, **695**, 1831–1837; (e) S. P. Nolan, H. Clavier, *Chem. Soc. Rev.*, 2010, **39**, 3305–3316.
16. (a) C. M. Moore, N. K. Szymczak, *Chem. Commun.*, 2013, **49**, 400–402; (b) K.-N. T. Tseng, J. W. Kampf, N. K. Szymczak, *Organometallics*, 2013, **32**, 2046–2049; (c) K.-N. T. Tseng, A. M. Rizzi, N. K. Szymczak, *J. Am. Chem. Soc.*, 2013, **135**, 16352–16355.
17. (a) D. K. Dutta, B. Deb, *Coord. Chem. Rev.*, 2011, **255**, 1686–1712; (b) C. S. Yi, *J. Organomet. Chem.*, 2011, **696**, 76–80; (c) I. Mellone, M. Peruzzini, L. Rosi, D. Mellmann, H. Junge, M. Beller, L. Gonsalvi, *Dalton Trans.*, 2013, **42**, 2495–2501.
18. (a) R. A. Leising, J. J. Grzybowski, K. J. Takeuchi, *Inorg. Chem.*, 1988, **27**, 1020–1025. (b) B. J. Coe, D. W. Thompson, C. T. Culbertson, J. R. Schoonover, T. J. Meyer, *Inorg. Chem.*, 1995, **34**, 3385–3395. (c) L. F. Szczepura, S. A. Kubow, R. A. Leising, W. J. Perez, M. H. V. Huynh, C. H. Lake, D. G. Churchill, M. R. Churchill, K. J. J. Takeuchi, *Chem. Soc., Dalton Trans.: Inorg. Chem.*, 1996, **7**, 1463–1470. (d) W. J. Perez, C. H. Lake, R. F. See, L. M. Toomey, M. R. Churchill, K. J. Takeuchi, C. P. Radano, W. J. Boyko, C. A. Bessel, *J. Chem. Soc., Dalton Trans.*, 1999, 2281–2292. (e) S. B. Billings, M. T. Mock, K. Wiacek, M. B. Turner, W. S. Kassel, K. J. Takeuchi, A. L. Rheingold, W. J. Boyko, C. A. Bessel, *Inorg. Chim. Acta*, 2003, **355**, 103–115. (f) S. Sharma, S. K. Singh, M. Chandra, D. S. Pandey, *J. Inorg. Biochem.*, 2005, **99**, 458–466. (g) C. M. Moore, N. K. Szymczak, *Chem. Commun.*, 2013, **49**, 400–402.
19. (a) B. P. Sullivan, D. J. Salmon, T. J. Meyer, *Inorg. Chem.*, 1978, **17**, 3334–3341. (b) B. P. Sullivan, D. Conrad, T. J. Meyer, *Inorg. Chem.*, 1985, **24**, 3640–3645. (c) J. P. Otruba, G. A. Neyhart, W. J. Dressick, J. L. Marshall, B. P. Sullivan, P. A. Watkins, T. J. Meyer, *J. Photochem.*, 1986, **35**, 133–153. (d) R. A. Leising, K. J. Takeuchi, *Inorg. Chem.*, 1987, **26**, 4391–4393. (e) R. A. Leising, J. S. Ohman, K. J. Takeuchi, *Inorg. Chem.*, 1988, **27**, 3804–3809. (f) C. A. Bessel, J. A. Margarucci, J. H. Acquaye, R. S. Rubmo, J. Crandall, A. J. Jircitano, K. J. Takeuchi, *Inorg. Chem.* 1993, **32**, 5779–5784. (g) M. R. Churchill, L. M. Krajkowski, M. H. V. Huynh, K. J. Takeuchi, *J. Chem. Crystallogr.*, 1997, **27**, 589–597. (h) M. Salierno, E. Marceca, D. S. Peterka, R. Yuste, R. Etchenique, *J. Inorg. Biochem.*, 2010, **104**, 418–422. (i) S. V. Litke, A. Y. Ershov, T. J. Meyer, *J. Phys. Chem. A*, 2011, **115**, 14235–14242. (j) V. S. Miguel, M. Álvarez, O. Filevich, R. Etchenique, A. del Campo, *Langmuir*, 2012, **28**, 1217–1221. (k) R. Araya, V. Andino-Pavlovsky, R. Yuste, R. Etchenique, *ACS Chem. Neurosci.*, 2013, **4**, 1163–1167.
20. (a) M. E. Marmion, K. J. Takeuchi *J. Chem. Soc., Dalton Trans.*, 1988, 2385–2391; (b) C. A. Bessel, R. A. Leising, K. J. Takeuchi, *J. Chem. Soc., Chem. Commun.*, 1991, 833–835; (c) N. D. Schley, G. E. Dobereiner, R. H. Crabtree, *Organometallics*, 2011, **30**, 4174–4179;
21. G. Nakamura, M. Okamura, M. Yoshida, T. Suzuki, H. D. Takagi, M. Kondo, S. Masaoka, *Inorg. Chem.*, 2014, **53**, 7214–7226.
22. J. Heinecke, P. C. Ford, *Coord. Chem. Rev.*, 2010, **254**, 235–247.
23. M. T. Gladwin, A. N. Schechter, D. B. Kim-Shapiro, R. P. Patel, N. Hogg, S. Shiva, R. O. Cannon III, M. Kelm, D. A. Wink, M. Graham Espey, E. H. Oldfield, R. M. Pluta, B. A. Freeman, J. R. Lancaster Jr., M. Feelisch, J. O. Lundberg, *Nat. Chem. Biol.*, **2005**, **1**, 308–314.
24. R. A. Leising, S. A. Kubow, K. J. Takeuchi, *Inorg. Chem.*, 1990, **29**, 4569–4574.
25. P. Singh, J. Fiedler, S. Zális, C. Duboc, M. Niemeyer, F. Lissner, T. Schleid, W. Kaim, *Inorg. Chem.*, 2007, **46**, 9254–9261.
26. (a) D. W. Pipes, T. J. Meyer, *Inorg. Chem.*, 1984, **23**, 2466–2472; (b) W. R. Murphy, Jr., K. J. Takeuchi, M. H. Barley, T. J. Meyer, *Inorg. Chem.*, 1984, **25**, 1041–1053.
27. R. G. de Lima, M. G. Sauaia, D. Bonaventure, A. C. Tedesco, L. M. Bendhack, R. S. da Silva, *Inorg. Chim. Acta*, 2006, **359**, 2543–2549.
28. A. Altomare, G. Cascarano, C. Giacovazzo, A. J. Guagliardi, *J. Appl. Cryst.*, 1993, **26**, 343–350.
29. G. M. Sheldrick, *Acta Crystallogr. Sect. A*, 2008, **64**, 112–122.
30. L. J. Farrugia, *J. Appl. Crystallogr.*, 1997, **30**, 565–566.
31. T. D. Fenn, D. Ringe, G. A. Petsko, *J. Appl. Crystallogr.*, 2003, **36**, 944–947.
32. M. J. Frisch, G. W. Trucks, H. B. Schlegel, G. E. Scuseria, M. A. Robb, J. R. Cheeseman, G. Scalmani, V. Barone, B. Mennucci, G. A. Petersson, H. Nakatsuji, M. Caricato, X. Li, H. P. Hratchian, A. F. Izmaylov, J. Bloino, G. Zheng, J. L. Sonnenberg, M. Hada, M. Ehara, K. Toyota, R. Fukuda, J. Hasegawa, M. Ishida, T. Nakajima, Y. Honda, O. Kitao, H. Nakai, T. Vreven, J. A. Montgomery, Jr. J. E. Peralta, F. Ogliaro, M. Bearpark, J. J. Heyd, E. Brothers, K. N. Kudin, V. N. Staroverov, T. Keith, R. Kobayashi, J. Normand, K. Raghavachari, A. Rendell, J. C. Burant, S. S. Iyengar, J. Tomasi, M. Cossi, N. Rega, J. M. Millam, M. Klene, J. E. Knox, J. B. Cross, V. Bakken, C. Adamo, J. Jaramillo, R. Gomperts, R. E. Stratmann, O. Yazyev, A. J. Austin, R. Cammi, C. Pomelli, J. W. Ochterski, R. L. Martin, K. Morokuma, V. G. Zakrzewski, G. A. Voth, P. Salvador, J. J. Dannenberg, S. Dapprich, A. D. Daniels, O. Farkas, J. B. Foresman, J. V. Ortiz, J. Cioslowski, D. J. Fox, *Gaussian 09 (Revision C.01)*, Gaussian, Inc. Wallingford CT, 2010.
33. A. D. Becke, *J. Chem. Phys.*, 1993, **98**, 5648–5652;
34. C. Lee, W. Yang, R. G. Parr, *Phys. Rev. B*, 1988, **37**, 785–789.
35. (a) T. H. Dunning, Jr. P. J. Hay, in *Modern Theoretical Chemistry*, ed. H. F. Schaefer, III, Plenum, New York, 1976; (b) P. J. Hay, W. R. Wadt, *J. Chem. Phys.*, 1985, **82**, 270–283; (c) P. J. Hay, W. R. Wadt, *J. Chem. Phys.*, 1985, **82**, 299–310. (d) D. Andrae, U. Haeussermann, M. Dolg, H. Stoll, H. Preuss, *Theor Chim Acta* 1990, **77**, 123.

36. M. Cossi, G. Scalmani, N. Rega, V. Barone, *J. Chem. Phys.*, 2002, **117**, 43–54.
37. (a) M. E. Casida, C. Jamorski, K. C. Casida, D. R. Salahub, *J. Chem. Phys.*, 1998, **108**, 4439–4449; (b) R. E. Stratmann, G. E. Scuseria, M. J. Frisch, *J. Chem. Phys.*, 1998, **109**, 8218–8224; (c) R. Bauernschmitt, R. Ahlrichs, *Chem. Phys. Lett.*, 1996, **256**, 454–464.
38. P. T. Burks, J. V. Garcia, R. GonzalezIrias, J. T. Tillman, M. Niu, A. A. Mikhailovsky, J. Zhang, F. Zhang, P. C. Ford, *J. Am. Chem. Soc.*, 2013, **135**, 18145–18152.
39. (a) J. G. Calvert, J. N. Pitts, *Photochemistry*; J. Wiley & Sons: New York, 1967; pp 783–786. (b) G. Malouf, P. C. Ford, *J. Am. Chem. Soc.*, 1977, **99**, 7213–7221.
40. C. F. Works, C. J. Jocher, G. D. Bart, X. Bu, P. C. Ford, *Inorg. Chem.*, 2002, **41**, 3728–3739.

ARTICLE

Graphical Abstract

Four novel phosphine-substituted ruthenium(II) polypyridine complexes with nitrogen oxides were synthesised and structurally characterized by single-crystal X-ray structural analysis. The substitution lability of the nitrogen oxide ligand of each complex is discussed in comparison with that of the corresponding acetonitrile complexes.

